Metallothioneins 1 and 2 Attenuate Peroxynitrite-Induced Oxidative Stress in Parkinson Disease

MANUCHAIR EBADI*,[1] AND SUSHIL SHARMA†

Departments of Pharmacology and Clinical Neurosciences; and †the Center of Excellence in Neurosciences, Cyclotron and Positron Imaging Research Laboratory, University of North Dakota School of Medicine and Health Sciences, Grand Forks, North Dakota 58202

We have examined potent peroxynitrite ion ($ONOO^-$) generator 3-morpholinosydnonimine (SIN-1)–induced neurotoxicity in control wild-type ($control_{wt}$) mice, metallothionein double knockout (MT_{dko}) mice, metallothionein-transgenic (MT_{trans}) mice, and in cultured human dopaminergic (SK-N-SH) neurons to determine the neuroprotective potential of metallothionein against ONOO - induced neurodegeneration in Parkinson disease (PD). SIN-1–induced lipid peroxidation, reactive oxygen species synthesis, caspase-3 activation, and apoptosis were attenuated by metallothionein gene overexpression and augmented by metallothionein gene down-regulation. A progressive nigrostriatal dopaminergic neurodegeneration in weaver mutant (wv/wv) mice was associated with enhanced nitrite ion synthesis, metallothionein down-regulation, and significantly reduced dopamine synthesis and ^{18}F-DOPA uptake as determined by high-resolution micropositron emission tomography neuroimaging. The striatal ^{18}F-DOPA uptake was significantly higher in MT_{trans} mice than in MT_{dko} and α-synuclein knockout ($α\text{-}Syn_{ko}$) mice. These observations provide further evidence that nitric oxide synthase activation and $ONOO^-$ synthesis may be involved in the etiopathogenesis of PD, and that metallothionein gene induction may provide neuroprotection. Exp Biol Med 231:1576–1583, 2006

Key words: metallothioneins; 3-morpholinosydnonimine; $ONOO^-$; α-synuclein; dopamine; caspase-3; apoptosis; transplantation; ^{18}F-DOPA; Parkinson disease

Introduction

Parkinson disease (PD) is the second-most prevalent neurodegenerative disorder after Alzheimer disease (AD), affecting approximately 1% of the aging population beyond age 50 years. Selective neurodegeneration of nigrostriatal dopaminergic (NS-DA-ergic) neurons is manifested as muscular rigidity, facial twitches, postural irregularity, and body tremors in PD. The associated brain stem neurons of these patients are decorated with α-synuclein (α-Syn)–positive Lewy bodies, a hallmark of PD diagnosis (1). Recently, point mutations in the α-Syn gene at chromosome 4 have been discovered, which induce a familial type L-DOPA–responsive Parkinsonism. A significant down-regulation of mitochondrial complex-1 (ubiquinone-NADH-oxidoreductase) has been reported in a majority of patients with PD. Furthermore, significantly reduced glutathione in the substantia nigra enhances the risk of free radical (mainly $OH^•$) overproduction, leading to neuronal damage in PD.

Recent studies have shown that nitric oxide (NO) plays a critical role in mediating neurotoxicity associated with mitochondrial damage (4) and various neurological disorders such as stroke, PD, and dementia associated with human immunodeficiency virus (2, 3). 1-Methyl, 4-phenyl, 1,2,3,6-tetrahydropyridine (MPTP)–induced neurotoxicity is associated with microglial inducible nitric oxide synthase (iNOS) induction, hence inhibition of iNOS may be a promising target for the treatment of PD (5). Following administration of MPTP to mice, there was a robust gliosis in the substantia nigra pars compacta associated with significant up-regulation of iNOS. These changes preceded or paralleled MPTP-induced DA-ergic neurodegeneration. Mutant mice lacking the iNOS gene were comparatively more resistant to MPTP than their wild-type littermates, suggesting that iNOS is important in MPTP neurotoxicity, hence inhibitors of iNOS may provide a protective role in the treatment of PD (2). The other important contributing factors in the neuronal demise are abnormal activation of NOS and NO in the substantia nigra of patients with PD. Because the involvement of oxidative and nitrative stress is now being advocated in the etiopathogenesis of PD, a detailed study is needed to explore the precise molecular mechanism of NO-mediated neurodegeneration and metallothionein (MT)-induced neuroprotection in PD. Recently,

This research was supported by the National Institutes of Health grants 2R01 NS 34566-09 and 1R01 AG 17059-06, and by grant DATMO5-02C-1252 from the Counter Drug Technology Assessment Center, Office of National Drug Control Policy to M.E.

[1] To whom correspondence should be addressed at University of North Dakota School of Medicine and Health Sciences, 501 North Columbia Road, Grand Forks, ND 58203. E-mail: mebadi@medicine.nodak.edu

1535-3702/06/2319-1576$15.00

we discovered that MT gene overexpression in the brain of MT transgenic (MT_{trans}) mice inhibits nitration of α-synuclein and preserves mitochondrial coenzyme Q_{10} (CoQ_{10}) levels to afford neuroprotection against oxidative and nitrative stress of aging brain (6–13).

3-Morpholinosydnonimine (SIN-1) is a vasorelaxant, soluble guanyl cyclase stimulator, and a potent peroxynitrite ion generator, and produces not only oxidative stress, but also nitrative stress in DA-ergic neurons, hence it might play an important role in understanding the etiopathogenesis of PD. Therefore, we have now investigated the extent of neuroprotection afforded by MTs against SIN-1–induced apoptosis in a human dopaminergic (SK-N-SH) cell line. Our studies have shown that SIN-1–induced lipid peroxidation, reactive oxygen species (ROS) synthesis, caspase-3 activation, and apoptosis are attenuated by MT overexpression in SK-N-SH neurons. Transfection of SK-N-SH neurons with MT-1sense oligonucleotides inhibits SIN-1 apoptosis, whereas with MT-1antisense oligonucleotides SIN-1 apoptosis is accentuated. Furthermore, progressive NS-DA-ergic neurodegeneration in weaver mutant (wv/wv) mice is associated with increased striatal nitrite ion synthesis and MT down-regulation, and significantly reduced dopamine synthesis and ^{18}F-DOPA uptake. At any given age the striatal nitrite ion synthesis remained attenuated in MT_{trans} mice as compared with control ($control_{wt}$), MT double knockout (MT_{dko}), and α-Syn knockout ($\alpha\text{-}Syn_{ko}$) mice, indicating the neuroprotective potential of MTs in PD.

Materials and Methods

Animals. Experimental animals were housed in temperature- and humidity-controlled rooms with 12-hr day and night cycles, and were provided with commercially prepared chow and water *ad libitum*. The animals were acclimated to laboratory conditions for at least 4 days prior to experimentation. Care was taken to avoid any distress to animals during the period of experimentation. Breeder pairs of $control_{wt}$ C57BL/6J, MT_{dko}, MT_{trans}, $\alpha\text{-}Syn_{ko}$, and homozygous wv/wv mice were purchased from the Jackson Laboratory (Minneapolis, MN). Detailed information regarding these genotypes is available from the Jackson Laboratory Web page (www.jax.org/jaxmice). The breeder colony was maintained in an air-conditioned animal house facility in high-efficiency particulate air-filtered cages with free access to water and lab chow. The zinc, copper, and iron contents in the lab chow were monitored by atomic absorption spectrometry to maintain their adequate supply. Polymerase chain reaction analysis of the tail DNA was performed for genotyping.

Equipment. An RDS-111 cyclotron was purchased from CTI Molecular Imaging, Inc. (Knoxville, TN). BBS2V for $^{18}F_2$ delivery and Manuela Hot cell for dose calibration and dose fractionation were purchased from Comcer (Castelbolognese, Italy). A GINA Star ^{18}F-DOPA synthesis module was purchased from Raytest (Isotopenmessgerate GmbH, Straubenhardt, Germany). A high-performance liquid chromatography (HPLC) system for ^{18}F-DOPA quality control was purchased from Agilent Technologies (Böblinger, Germany). A high-resolution micropositron emission tomography (microPET) scanner (R4) was purchased from Concorde Microsystems (Knoxville, TN).

Chemicals. MT-1 and MT-2 standards, thiobarbituric acid, trichloroacetic acid, Griess reagent, and monoamine standards were purchased from Sigma Chemical Co. (St. Louis, MO). A caspase-3 assay kit was purchased from Pharmingen, Becton-Dickinson (Palo Alto, CA). 2′-7′-Dichlorofluorescein diacetate, 5,5′,6,6′-tetrachloro-1,1′, 3,3′-tetraethyl-benzimidazolylcarbocyanide iodide (JC-1), Annexin-V, and 4′,6′-diamidino-2-phenylindole dihydrochloride (DAPI) were purchased from Molecular Probes (Eugene, OR). Plastic ware for cell culture, Dulbecco modified Eagle medium (DMEM), fetal bovine serum (FBS), Dulbecco phosphate buffered saline pH 7.4 (d-PBS), and metallothionein (MT-1) oligonucleotide sequences for cell transfection were purchased from GIBCO-BRL Life Technologies (Rockville, MD). Sodium dihydrogen phosphate (NaH_2PO_4), ethanol, diammonium hydrogen phosphate ($(NH_4)_2HPO_4$, ammonium dihydrogen phosphate ($NH_4H_2PO_4$) ammonium hydroxide (NH_4OH), hydrobromic acid (HBr), and trichlorofluromethane (Freon), and ascorbic acid were purchased from Aldrich Chemicals (St. Louis, MO). Tri-boc, trimethylstannyl L-dihydroxylphenylalanine (precursor), and cold F-DOPA were purchased from Advanced Biochemical Compounds (ABX, GmbH, Radeberg, Germany). $^{18}O_2$ gas was purchased from Isotec (Miamisburg, OH).

Methods. The animals were sacrificed by decapitation. Twenty-five milligrams of the striatal tissue was homogenized in 1 ml of d-PBS at 4°C. One hundred microliters of the striatal homogenate was used for determining lipid peroxidation, ROS synthesis, caspase-3 activation, nitrite synthesis, and dopamine synthesis following SIN-1 intoxication as described in the figure legends. Cell transfection with MT-1 oligonucleotides was performed by using the cell transfection kit according to the manufacturer's instructions. A detailed description of cell transfection is provided in our recent publication (14, 15).

Lipid Peroxidation. The cells were grown in 12-well plates for 72 hrs. Fresh medium was added to examine the effect of SIN-1 or MT-1 (100 n*M*) (or both) overnight as described in the text. The cells were harvested and suspended in d-PBS, sonicated at low wattage for 30 secs, and 1 ml of thiobarbituric acid reagent (composition: 15% trichloroacetic acid, 0.375% thiobarbituric acid, and 0.25 *N* hydrochloric acid) was added. The samples were heated for 20 mins at 95°C, cooled in running ice-cold water, and centrifuged at 10,000 *g* for 10 mins. The optical density was measured at 535 nm using a microtiter plate reader.

ROS Synthesis. ROS synthesis was estimated spectrofluorometrically using 2′,7′-dichlorofluorescein diacetate as described in our previous publication (16).

Caspase-3 Activation. Caspase-3 activity was measured spectrofluorometrically using caspase-3–specific substrate AC-DEVD-AMC and inhibitor AC-DEVD-CHO as described in our previous publication (14).

Apoptosis. The cells were grown in polylysine-coated multichambered slides using complete DMEM supplemented with 10% FBS, 3.7 g/l sodium bicarbonate, high glucose, and glutamine. After 48 hrs of incubation at 37°C in a 5% CO_2 incubator, they were washed three times with d-PBS. They were then incubated in JC-1 (5 n*M*) for 30 mins at 37°C, washed three times, and counterstained with DAPI and ethidium bromide (5 n*M*) for 30 sec, and again washed three times in PBS. The slides were mounted in Fluor-Mounting Medium (Trevigen) and allowed to dry at room temperature in a dark chamber. The slides were examined with a digital fluorescence microscope (Leeds Instruments Co., Minneapolis, MN) set at three wavelengths. The fluorescence images were captured using a SpotLite digital camera and analyzed with ImagePro software. Target accentuation and background inhibition software were employed to improve the quality of fluorescent images as described in our recent publications (8, 11–15).

Nitrite Ion Estimation. The nitrite ion synthesis was estimated by using Griess reagent and a colorimetric microtiter plate reader according to the manufacturer's instructions.

Striatal Dopamine. The striatal dopamine was estimated from 25 mg of tissue by using HPLC with electrochemical detector (HPLC-EC) in an isocratic mode as described in our recent publication (17).

^{18}F-DOPA Synthesis. ^{18}F-DOPA synthesis required a single reaction vessel and involved two synthesis steps: (i) electrophilic substitution and (ii) fluorodestannlyzation. A detailed procedure is described in our recent publication (17). Briefly, all the ^{18}F-DOPA synthesis steps were computer-controlled and were performed remotely from the cyclotron and the Hot cells. The reagent vessels were filled with the following chemicals in sequence: Vessel 1: 3.5 ml of precursor (30 mg triboc, trimethylstannyl L-dihydroxylphenylalanine in Freon); Vessel 2: 48% of 1.8 ml hydrobromic acid (HBr); Vessel 3: 1.2 ml buffer (composition: $(NH_4)_2HPO_4$ [1 *M*] + $NH_4H_2PO_4$ [1 *M*] [50/50]); and Vessel 4: 1.1 ml of 25% NH_4OH. The RDS-111 cyclotron was initialized for the first 20 mins by employing Supervisory Control & Documentation Analysis (SCADA) computer commands via a Virtual Memory EuroBus (VME) Crate. The precursor was cooled in Freon down to –20°C within 10 mins to trap the entire $^{18}F_2$. The reaction vessel was then heated to 30°C for 4 mins, and Freon was evaporated under vacuum at 50°C, after which HBr was added to the residue. The reaction mixture was now heated to 130°C for 10 mins and then cooled to 70°C for 1 min and was neutralized by adding NH_4OH. The reaction vessel was further cooled to 40°C, and the buffer was added to adjust the pH to 4. The resulting solution was trapped in an HPLC injection loop (4.5 ml), automatically injected, and separated by an HPLC reverse-phase column (Nucleosil 100 C18, 7 μ*M*, 16 × 250 mm) using 2% ethanol in 0.5 *M* NaH_2PO_4 (pH 4–5), at a flow rate of 8 ml/min. The eluant was monitored for UV absorbance (282 nm) and radioactivity.

^{18}F-DOPA Uptake. The animals were anesthetized ip with 1.6-mg tribromoethane per gram of body weight. ^{18}F-DOPA uptake was studied by injecting 250 μCi of ^{18}F-DOPA iv through the caudal vein and high-resolution microPET scanning after 60 mins. The uptake of ^{18}F-DOPA in the striatal region was collected in list mode by microPET-Manager and quantitated by ASIPro computer software. The target (striatum) to nontarget (cerebellum) ratios of ^{18}F-DOPA uptake were determined by dissolving 10 mg of tissue in 1 *N* NaOH at 80°C and counting the radioactivity in a well-type gamma scintillation counter above background. A detailed procedure of ^{18}F-DOPA uptake is described in our recent publications (12, 18).

Statistical Analysis. The data were analyzed with Sigma-Stat (version 3.02), employing repeated measures ANOVA. *P* values less than 0.05 were taken as statistically significant.

Results

MTs Inhibit SIN-1–Induced Lipid Peroxidation. SIN-1–induced lipid peroxidation was significantly ($P < 0.05$) attenuated in MT_{trans} mice striatum as compared with $control_{wt}$, MT_{dko}, and α-Syn_{ko} mice (Fig. 1, left panel). Pretreatment with MT-1 (100 n*M*) also significantly reduced the SIN-1–induced increase in lipid peroxidation. SIN-1–induced lipid peroxidation was attenuated in MT-1sense oligonucleotide-transfected SK-N-SH neurons and was accentuated in MT-1antisense oligonucleotide-transfected neurons. Transfection with MT-1scrambled sequences did not induce a significant change in lipid peroxidation when compared with $control_{wt}$ neurons as presented in Figure 1 (right panel).

MTs Inhibit SIN-1–Induced ROS synthesis. SIN-1–induced ROS was significantly ($P < 0.01$) attenuated in MT_{trans} mice striatum as compared with $control_{wt}$, MT_{dko}, and α-Syn_{ko} mice (Fig. 2, left panel). Pretreatment with MT-1 (100 n*M*) also significantly reduced the SIN-1–induced increase in ROS synthesis. SIN-1–induced ROS synthesis was attenuated in MT-1sense oligonucleotide–transfected SK-N-SH neurons and was accentuated in MT-1antisense oligonucleotide–transfected neurons. Transfection with MT-1scrambled sequences did not induce a significant change in ROS synthesis when compared with $control_{wt}$ neurons as presented in Figure 2 (right panel).

MTs Inhibit SIN-1–Induced Caspase-3 Activation. SIN-1–induced caspase-3 activation was significantly ($P < 0.01$) attenuated in MT_{trans} mice striatum as compared with $control_{wt}$, MT_{dko}, and α-Syn_{ko} mice (Fig. 3, left panel).

Pretreatment with MT-1 (100 n*M*) also significantly reduced the SIN-1–induced increase in caspase-3 activation.

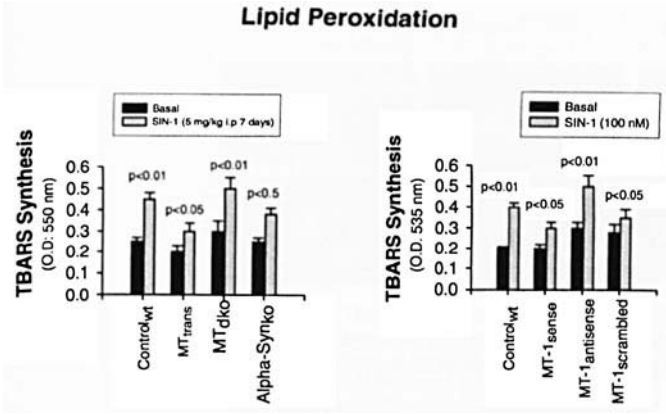

Figure 1. Left panel: A histogram representing SIN-1–induced lipid peroxidation in control$_{wt}$, MT$_{trans}$, MT$_{dko}$, and α-Syn$_{ko}$ mice striatum. Right panel: A histogram representing SIN-1–induced lipid peroxidation in control$_{wt}$, MT-1sense, MT-1antisense, and MT-1antisense-transfected SK-N-SH neurons. Data are mean ± SD of eight determinations in each experimental group.

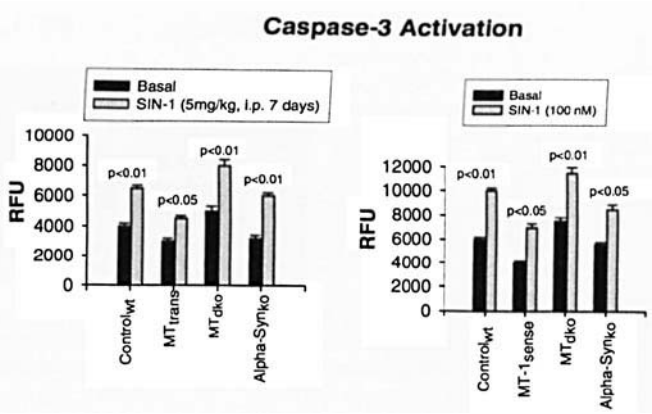

Figure 3. Left panel: A histogram representing SIN-1–induced caspase-3 activation in control$_{wt}$, MT$_{trans}$, MT$_{dko}$, and α-Syn$_{ko}$ mice striatum. Right panel: A histogram representing SIN-1–induced caspase-3 activation in control$_{wt}$, MT-1sense, MT-1antisense, and MT-1antisense–transfected SK-N-SH neurons. Data are mean ± SD of eight determinations in each experimental group.

SIN-1–induced caspase-3 activation was attenuated in MT-1sense oligonucleotide–transfected SK-N-SH neurons and was accentuated in MT-1antisense oligonucleotide–transfected neurons. Transfection with MT-1scrambled sequences did not induce a significant change in caspase-3 activation when compared with control$_{wt}$ neurons as presented in Figure 3 (right panel).

MTs Inhibit SIN-1 Apoptosis. Overnight treatment of SIN-1 induced apoptosis in control$_{wt}$ neurons. SIN-1 apoptosis was attenuated in MT-1sense oligonucleotide–transfected neurons and accentuated in MT-1antisense oligonucleotide–transfected neurons. Transfection with MT-1scrambled oligonucleotides did not induce a significant change in SIN-1 apoptosis (Fig. 4).

Overnight MT-1sense Treatment of SIN-1 Induces Apoptosis in Control$_{wt}$ Neurons. SIN-1 apoptosis was attenuated in MT-1sense oligonucleotide–transfected neurons and accentuated in MT-1antisense oligonucleotide–transfected neurons without any significant change in MT-1scrambled oligonucleotide–transfected neurons, indicating the neuroprotective potential of MTs in peroxynitrite-mediated neurodegeneration.

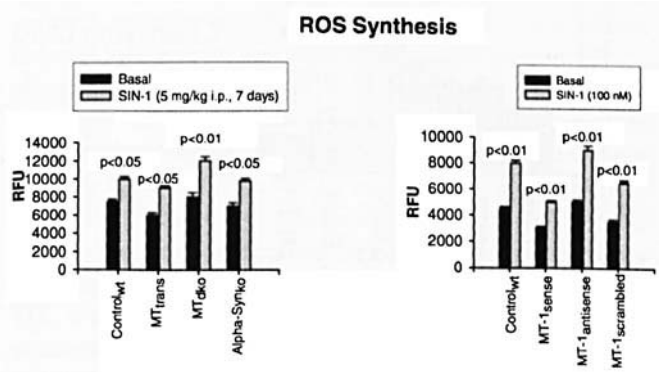

Figure 2. Left panel: A histogram representing SIN-1–induced ROS synthesis in control$_{wt}$, MT$_{trans}$, MT$_{dko}$, and α-Syn$_{ko}$ mice striatum. Right panel: A histogram representing SIN-1–induced ROS synthesis in control$_{wt}$, MT-1sense, MT-1antisense, and MT-1antisense–transfected SK-N-SH neurons. Data are mean ± SD of 10 determinations in each experimental group.

MTs Inhibit Nitrite Synthesis. The synthesis of the striatal nitrite ions was significantly ($P < 0.01$) increased in the wv/wv mice as compared with other experimental groups. The striatal nitrite ion formation in the 45-day-old mice from control$_{wt}$, MT$_{trans}$, MT$_{dko}$, wv/wv, and α-Syn$_{ko}$ mice is presented in Figure 5A. The nitrite ion formation increased with age in wv/wv mice (Fig. 5B). A progressive increase in the striatal nitrite ion formation was noticed exclusively in wv/wv mice exhibiting progressive nigrostriatal DA-ergic neurodegeneration. The other experimental groups neither exhibit progressive nitrite formation nor DA-ergic degeneration as observed in wv/wv mice. A progressive reduction in the striatal dopamine was observed in aging wv/wv mice (Fig. 5C). A negative correlation between the striatal nitrite and dopamine synthesis was observed as a function of aging in wv/wv mice with a correlation coefficient of 0.94 (Fig. 5D).

MTs Enhance CoQ_{10} Synthesis. To authenticate that MTs provide CoQ_{10}-mediated neuroprotection, we treated MT mice with chronic MPTP (30 mg/kg, ip) for 7 days and estimated striatal CoQ_{10} levels. Basal levels of CoQ_9 were not significantly affected in the control$_{wt}$, MT$_{dko}$, or MT$_{trans}$ mice. Following chronic MPTP administration, striatal CoQ_{10} remained elevated in MT$_{trans}$ mice and was significantly reduced in MT$_{dko}$ mice (Fig. 6). This was reflected as severe Parkinsonism in MT$_{dko}$ mice as compared with MT$_{trans}$ mice.

MTs Enhance Dopamine Synthesis. The striatal dopamine synthesis was not significantly different in MT$_{trans}$, MT$_{dko}$, or α-Syn$_{ko}$ mice as compared with control$_{wt}$ mice; however, a significant reduction in striatal dopamine was observed in the wv/wv mice as compared with control$_{wt}$ and other experimental groups as shown in Figure 7.

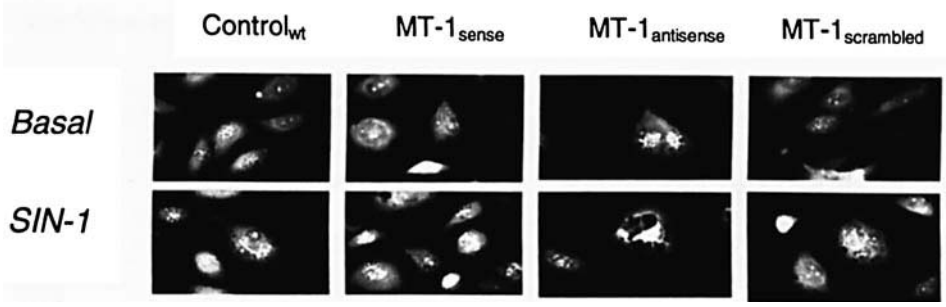

Figure 4. Multiple fluorochrome digital fluorescence imaging analysis of SIN-1 apoptosis in control$_{wt}$, MT-1sense, MT-1antisense, and MT-1scrambled oligonucleotide–transfected SK-N-SH neurons. Fluorochromes: red, JC-1 (mitochondrial membrane potential [$\Delta\Psi$] marker); blue, DAPI (nuclear DNA stain); green, (fluorescein isothiocyanate-conjugated antiphosphatidyl serine antibody, Annexin-V).

^{18}F-DOPA Uptake versus Striatal MTs. ^{18}F-DOPA uptake was significantly reduced in the central nervous system of wv/wv mice due to down-regulation of MTs in aging wv/wv mice. The striatal MT levels were significantly ($P < 0.05$) reduced in aging wv/wv mice exhibiting progressive dopaminergic neurodegeneration and neurobehavioral abnormalities. The striatal MTs were 10 ± 3 ng/mg protein in control$_{wt}$ mice and 6 ± 2 ng/mg protein in 120-day-old wv/wv mice as determined by colorimetric enzyme-linked immunosorbent assay. Mice of the wv/+ type did not exhibit any significant change in striatal MT when compared with control$_{wt}$ mice. Reduction in the striatal MT ran concomitantly with significantly reduced ^{18}F-DOPA uptake in aging wv/wv mice. Representative microPET neuroimages at the striatal level illustrating normal ^{18}F-DOPA uptake in control$_{wt}$ and wv/+ mice as compared with wv/wv mice are presented in Figure 8.

Discussion

We have now provided evidence that MT gene overexpression could suppress the $ONOO^-$ ion generator, SIN-1–induced neurodegeneration in DA-ergic neurons in order to provide neuroprotection in PD. Hence, antiparkinsonian drugs could be targeted to enhance the brain regional molecular induction of MTs. SIN-1–induced lipid peroxidation, ROS synthesis, caspase-3 activation, and apoptosis were attenuated by MT gene overexpression. These observations were authenticated using MT$_{trans}$, MT$_{dko}$, and α-Syn$_{ko}$ mice. Further confirmation was sought by trans-

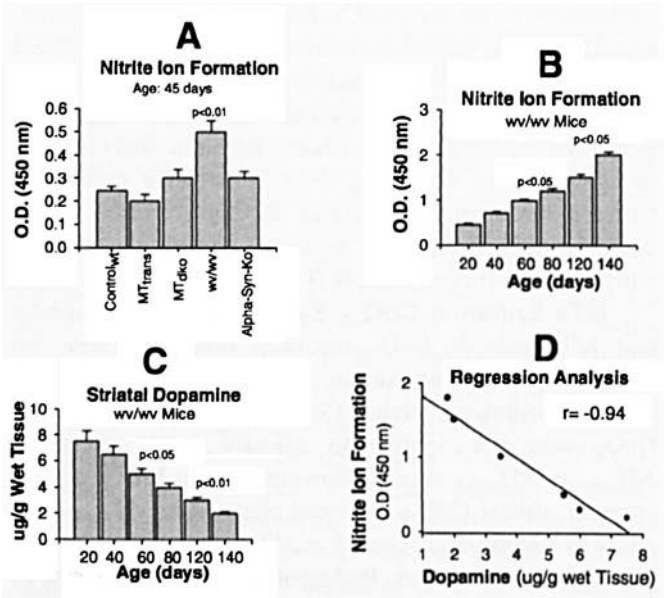

Figure 5. (A) A histogram representing quantitative estimates of the striatal nitrite ion formation to authenticate our hypothesis that MTs provide CoQ_{10}-mediated neuroprotection. (B) A histogram representing an age-dependent increase in the nitrite ion formation in wv/wv mice. (C) A histogram representing a reduction in the striatal dopamine as a function of aging in wv/wv mice. (D) Regression analysis demonstrating a negative correlation between striatal dopamine synthesis and nitrite ion formation in wv/wv mice. Data are mean ± SD of eight determinations in each experimental group.

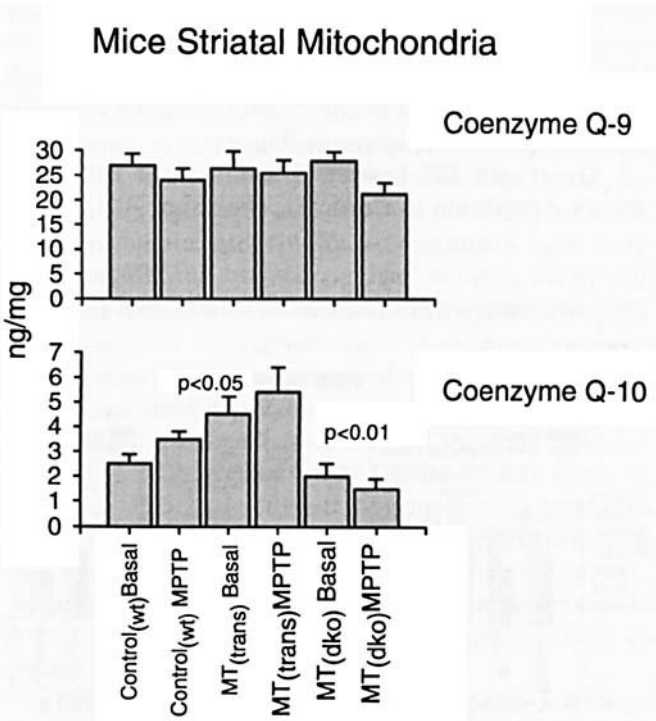

Figure 6. Histograms representing significantly reduced CoQ_{10} in MT$_{dko}$ mice striatal mitochondria as compared with that in MT$_{trans}$ mice in response to chronic MPTP (30 mg/kg, ip for 7 days). CoQs were estimated using HPLC with UV detection at 275 nm and hexane:methanol (1:3) mobile phase. Data are mean ±SD of eight determinations in each group.

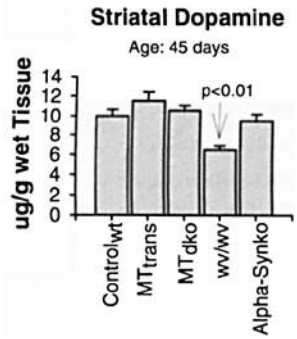

Figure 7. A histogram demonstrating quantitative analysis of the striatal dopamine from different experimental groups exhibiting no significant difference when compared with control$_{wt}$ mice. The striatal dopamine is significantly ($P < 0.05$) reduced in wv/wv mice. Data are mean ± SD of eight determinations in each experimental group.

fecting the SK-N-SH neuron with sense, antisense, and scrambled oligonucleotides of MT-1. These observations lend further support to previous observations by Cai *et al.* (19) and our recent observations (12, 14, 15).

Although the precise molecular mechanism of MT-mediated neuroprotection remains enigmatic, we have proposed that MTs provide neuroprotection from $ONOO^-$ by augmenting CoQ_{10} synthesis. The striatal CoQ_{10} remained elevated in MT_{trans} mice as compared with MT_{dko} mice even after chronic treatment of MPTP, which induces $ONOO^-$ synthesis in rodents (10–14). MT_{trans} mice were genetically resistant to MPTP as compared with MT_{dko} mice, suggesting that MTs offer neuroprotection in PD (8, 14, 15). These observations provide further evidence that MTs provide CoQ_{10}-mediated neuroprotection in PD. Furthermore, MTs suppress SIN-1–induced $ONOO^-$ synthesis by donating zinc ions. Zinc released from MT participates in NOS inhibition and prevents $ONOO^-$ synthesis, whereas 6-OH-DA, by donating hydroxyl radicals, may react with NO to synthesize $ONOO^-$. Chronic MPTP enhances NOS activity in the mouse striatum (20). NO reacts readily with superoxide ion to synthesize $ONOO^-$ ions. Zinc inhibits NOS activity and protects DA-ergic neurons from $ONOO^-$ ions during MPTP or rotenone-induced oxidative and nitrative stress. MPTP and rotenone-induced zinc release was significantly increased in MT_{trans} mice as compared with that in MT_{dko} mice, indicating that MTs may inhibit $ONOO^-$ by donating zinc, whereas the oxidized form of iron may participate in a Fenton reaction to generate OH radicals in MT_{dko} mice. The hydroxyl radicals may react with NO to synthesize $ONOO^-$ ions. Because MTs regulate the intracellular redox potential, we explored whether or not 6-OH-DA could alter the level of zinc and MT. 6-OH-DA reduced the levels of zinc and MT in the striatum but not in other brain regions. The effect of DA in stimulating the synthesis of MTs was similar to that of zinc, which is known to generate the synthesis of MT, and to that of H_2O_2 and $FeSO_4$, which is known to generate free radicals, indicating that zinc or zinc MTs are altered in conditions in which oxidative stress has taken place (21).

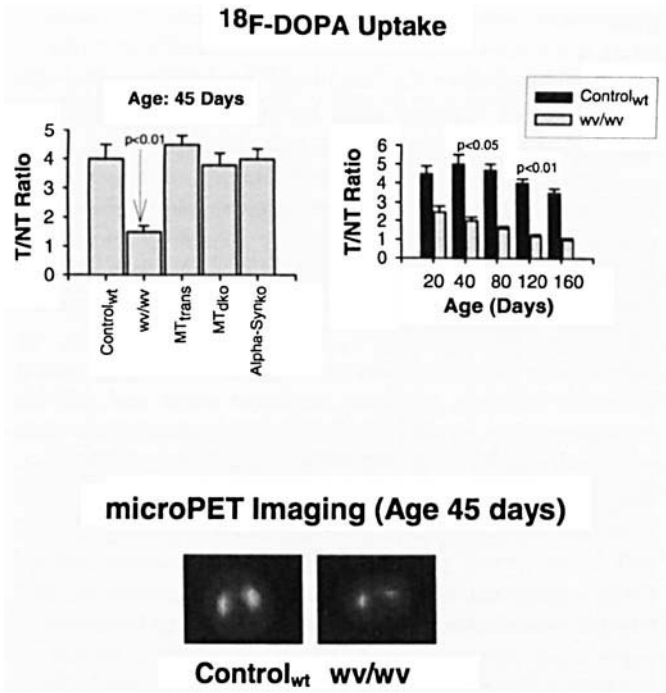

Figure 8. Upper left panel: A histogram representing target (striatum) to nontarget (cerebellar) ratios of ^{18}F-DOPA uptake from 45-day-old control$_{wt}$, wv/wv, MT_{trans}, MT_{dko}, and α-Syn_{ko} mice. Data are mean ± SD of eight determinations in each experimental group. ^{18}F-DOPA uptake was significantly ($P < 0.01$) reduced in wv/wv mice compared with other experimental genotypes. Upper right panel: A histogram representing quantitative estimate of progressive reduction in the target (striatum) to nontarget (cerebellar) ratio of ^{18}F-DOPA uptake in aging wv/wv mice. At any given age the T:NT ratio was significantly ($P < 0.05$) reduced in wv/wv mice as compared with control$_{wt}$ mice. Lower panel: A representative microPET neuroimage illustrating reduced ^{18}F-DOPA uptake in the striatal region of a wv/wv mouse as compared with a control$_{wt}$ mouse.

These observations were authenticated by local microinjections of the OH radical generators 6-OH-DA and SIN-1. Indeed, coadministration of 6-OH-DA with SIN-1 accentuated hemiparkinsonism (12).

Significantly reduced release of zinc in MT_{dko} mice might be responsible for the enhanced susceptibility to MPTP Parkinsonism, whereas in MT_{trans} mice these events are attenuated by an augmented release of zinc (12). Because $ONOO^-$ has been implicated in the etiopathogenesis of various neurodegenerative diseases, we investigated the neuroprotective role of MTs (14, 15, 22) in various cellular and genetic models of PD. MTs are expressed in neurons that sequester zinc in their synaptic vesicles. The regulation of the expression of MTs is extremely important in terms of maintaining the steady-state level of zinc and controlling redox potentials. Because several neurodegenerative disorders are associated with oxidative stress, and because MT is able to prevent the formation of free radicals and $ONOO^-$ ions, it is believed that cytokine-induced induction of MT provides a long-lasting protection to avert oxidative and nitrative damage (23). The mobilization of zinc from MT suggests a possible function of MT as a physiological zinc donor. A shift in the

glutathione redox balance under conditions of oxidative stress accelerates zinc release from MT. Such a disturbance in zinc metabolism has important consequences for the progression of diseases such as PD, in which oxidative stress occurs in affected brain tissue (24, 25).

Recently, we have reported that MT overexpression may protect DA-ergic neurons against salsolinol-induced neurotoxicity by the inhibition of oxidative stress and apoptotic pathways, including caspase-3 activation and α-Syn nitration (22). We have discovered that selegiline, by preventing the generation of free radicals; MTs, by scavenging free radicals; and neurotrophins, by rescuing DA-ergic neurons, attenuate oxidative stress and provide neuroprotection in PD (26, 27). Furthermore, we have proposed that MTs provide CoQ_{10}-mediated neuroprotection in PD (10). To authenticate this hypothesis, we used $control_{wt}$, MT_{dko}, MT_{trans}, $\alpha\text{-}Syn_{ko}$, and wv/wv mice. MT_{dko} and wv/wv mice possessed significantly reduced striatal CoQ_{10} compared with MT_{trans} and $\alpha\text{-}Syn_{ko}$ mice (8, 28). Chronic intoxication of rotenone also reduced complex-1 expression and increased NFκβ expression. NFκβ is induced in $ONOO^-$-induced oxidative and nitrative stress (16). MPTP, rotenone, salsolinol, 6-OH-DA, and SIN-1–induced α-Syn nitration was significantly suppressed in SK-N-SH neurons by MT induction (14, 15). Transfection of RhOmgko neurons with MT-1sense oligonucleotides also significantly increased CoQ_{10} and enhanced neuritogenesis, suggesting that MTs provide CoQ_{10}-mediated neuroprotection to avert $ONOO^-$ damage (8–13). We have also proposed that areas of the brain such as striatum, which contains high concentrations of iron but low levels of inducible MTs, are particularly vulnerable to oxidative stress (29–31).

SIN-1 can induce Bax up-regulation and BCl-2 down-regulation in DA-ergic neurons, whereas MT gene induction by its overexpression or through selegiline could afford neuroprotection (14).

$ONOO^-$ ions have been implicated in the progressive neurodegeneration in stroke, ischemia, Alzheimer disease, PD, multiple sclerosis, motor neuron disease, and inflammatory diseases (32) O_2^- produced by the reduction of O_2 has one unpaired electron, which can rapidly combine with the unpaired electron of NO to form $ONOO^-$. O_2^- levels are kept low by the enzyme superoxide dismutase (SOD), which dismutases O_2^- to H_2O_2 and O_2^-. SOD catalyzes the dismutation reaction of O_2^-; however, in the presence of H_2O_2, SOD can produce potentially damaging hydroxyl $OH^\cdot$ radicals, and high levels of SOD can be damaging to the cell (33). Nitration of protein tyrosine residues is a convenient marker of $ONOO^-$ production *in vivo* (34), and nitration of neurofilaments is enhanced by $ONOO^-$ (32). $ONOO^-$ is known to inhibit the mitochondrial electron transport chain (35). Therefore, overexpression of mitochondrial genome knockout aging DA-ergic neurons (RhOmgko) to mitochondrial genome encoding complex-1 activity significantly attenuated SIN-1–induced lipid peroxidation and caspase-3 activation, confirming the neuroprotective potential of MT gene overexpression. Selegiline pretreatment also exhibited similar neuroprotective influences when exposed to SIN-1–treated cells. Selegiline could produce neuroprotection through several possible molecular mechanisms (36). The most plausible mechanism or mechanisms of neuroprotection is through MT gene overexpression (37).

Recently, a genetically modified PC12 cell line that could synthesize nerve growth factor under the control of a zinc-inducible MT promoter has been developed. When implanted in the rat striatum and under *in vivo* zinc stimulation, these cells differentiated, expressed tyrosine hydroxylase, and survived through potential autocrine trophic support (38). Furthermore, MT overexpression in pancreatic β cells provided resistance to oxidative stress by scavenging ROS, including H_2O_2, $ONOO^-$ released from streptozotocin, SIN-1, and superoxide radical produced by xanthine/xanthine oxidase. MT reduced NO-induced β cell death and ROS production, and improved islet cell survival. MT islets synthesized more insulin than controls and extended the duration of euglycemia. The benefit of MT was due to protection from ROS because nitrotyrosine synthesis, an indicator of $ONOO^-$ synthesis, was much lower in MT grafts (39). Recently, we have reported that MT_{trans} fetal stem cells are resistant to dihydroxyphenyl acetaldehyde (DOPAL) apoptosis as compared with $control_{wt}$ cells (14), indicating their therapeutic potential in neuronal replacement therapy of PD. Because wv/wv mice exhibit progressive DA-ergic degeneration and MT_{trans} fetal stem cells are resistant to $ONOO^-$-induced apoptosis, MT_{trans} fetal stem cells may be used for transplantation in wv/wv mice. We are now evaluating the outcome of these grafts by high-resolution microPET imaging using ^{18}F-DOPA.

In conclusion, $ONOO^-$ ions are generated as a result of oxidative and nitrative stress, which induce lipid peroxidation, ROS synthesis, caspase-3 activation, apoptosis, and eventually degeneration of DA-ergic neurons in PD. MTs provide neuroprotection as an antioxidant through –SH moieties on the cysteine residues and by augmenting glutathione function (40, 41). MTs may also provide neuroprotection by donating, buffering, and scavenging zinc involved in the transcriptional regulation of several redox-sensitive genes and by inhibiting iNOS in PD. MTs enhanced CoQ_{10} synthesis to avert iNOS activity and provided neuroprotection by suppressing $ONOO^-$ synthesis. Because $ONOO^-$ is involved in graft rejection and MTs attenuate $ONOO^-$ apoptosis, MT_{trans} fetal stem cells can be implanted in wv/wv mice exhibiting increased nitrite ion synthesis, progressive DA-ergic degeneration, and Parkinsonism. Further studies in this direction will determine the basic molecular mechanism of graft acceptance/rejection in PD and the exact role of $ONOO^-$ in the etiopathogenesis of PD, which will go a long way in the clinical management of PD in the future.

We thank the employees of CTI Corporation, Comecer, and raytest for the success of this project.

1. Ebadi M, Pfeiffer R. Parkinson's Disease. London, England: Taylor and Francis, 2005.
2. Dawson VL, Dawson TM. Nitric oxide in neurodegeneration. Prog Brain Res 118:215–229, 1998.
3. Bredt DS. Endogenous nitric oxide synthesis: biological functions and pathophysiology. Free Radic Res 31:577–596, 1999.
4. Ghafourifar P, Colton C. Mitochondria and nitric oxide. Antiox Redox Signal 5:249–250, 2003.
5. Dehmer T, Lindenau J, Haid S, Dichgans J, Schulz JB. Deficiency of inducible nitric oxide synthase protects against MPTP toxicity in vivo. J Neurochem 74:2213–2216, 2001.
6. Sharma SK, Sangchot P, Ebadi M. Metallothionein gene manipulation influences striatal mitochondrial ubiquinones and MPTP-induced neurotoxicity in dopaminergic neurons. XIV World Congress of Pharmacology, July 7–12, 2002, San Francisco. 14:106–107, 2002.
7. Sharma SK, Shavali S, El Rafaey H, Ebadi M. Inhibition of α-synuclein nitration and perinuclear aggregation by antioxidants in metallothionein transgenic and aging RhO (mgko) dopaminergic neurons (abstract). FASEB J 16:686.11, 2002.
8. Sharma S, Kheradpezhou M, Shavali S, El Refaey H, Eken J, Hagen C, Ebadi M. Neuroprotective actions of coenzyme Q10 in Parkinson's disease. Methods Enzymol 382:488–509, 2004.
9. Ebadi M, Sharma SK. Mitochondrial α-synuclein-metallothionein interaction in Parkinson's disease. FASEB J 16:697.6, 2002.
10. Ebadi M, Sharma S, Muralikrishnan D, Shavali S, Josh E, Sangchot P, Chetsawang B, Brekke L. Metallothionein provides ubiquinone-mediated neuroprotection in Parkinson's disease. Proc West Pharmacol Soc 45:1–3, 2002.
11. Ebadi M, Brown-Borg H, El Refaey H, Singh B, Garrett S, Shavali S, Sharma SK. Metallothionein-mediated neuroprotection in genetically engineered mice models of Parkinson's disease. Mol Brain Res 134:67–75, 2005.
12. Ebadi M, Sharma SK, Ghafourifar P, Brown-Borg H, El Refaey H. Peroxynitrite in the pathogenesis of Parkinson's disease and the neuroprotective role of metallothioneins. Methods Enzymol 396:276–298, 2005.
13. Ebadi M, Sharma SK, Wanpen S, Shavali S. Metallothionein isoforms attenuate peroxynitrite-induced oxidative stress in Parkinson's disease. In: Ebadi M, Pfeiffer R, Eds. Parkinson's Disease. Boca Raton, FL: CRC Press, pp479–499, 2005.
14. Sharma SK, Ebadi M. Metallothionein attenuates 3-morpholinosydnonimine (SIN-1)-induced oxidative stress in dopaminergic neurons. Antioxid Redox Signal 5:251–264, 2003.
15. Ebadi M, Sharma S. Peroxynitrite and mitochondrial dysfunction in the pathogenesis of Parkinson's disease. Antioxid Redox Signal 5:319–335, 2003.
16. Sangchot P, Sharma S, Chetsawang B, Porter J, Govitrapong P, Ebadi M. Deferoxamine attenuates iron-induced oxidative stress and prevents mitochondrial aggregation and α-synuclein translocation in SK-N-SH cells in culture. Dev Neurosci 24:143–153, 2002.
17. Ebadi M, Sharma SK, Wanpen S, Amornpan A. Coenzyme Q10 inhibits mitochondrial complex-1 down-regulation and nuclear factor-kappa B activation. J Cell Mol Med 8:213–222, 2004.
18. Sharma SK, Ebadi M. Distribution kinetics of ^{18}F-DOPA in Weaver mutant mice. Mol Brain Res 139:23–30, 2005.
19. Cai L, Klein JB, Kang YJ. MT inhibits peroxynitrite-induced DNA and lipoprotein damage. J Biol Chem 275:38957–38960, 2001.
20. Halasz A, Palfi M, Tabi T, Magyar K, Szoko E. Altered nitric oxide production in mouse brain after administration of 1-methyl-4-phenyl-1,2,3,6-tetrahydropyridine or met-amphetamine. Neurochem Int 44: 641–646, 2004.
21. Shiraga H, Pfeiffer R, Ebadi M. The effects of 6-hydroxydopamine and oxidative stress on the level of brain metallothionein. Neurochem Int 23:561–566, 1993.
22. Wanpen S, Govitrapong P, Shavali S, Sangchot P, Ebadi M. Salsolinol, a dopamine-derived tetrahydroisoquinoline, induces cell death by causing oxidative stress in dopaminergic SH-S-Y5Y cells, and the said effect is attenuated by metallothionein. Brain Res 1005:67–76, 2004.
23. Ebadi M, Iversen P, Hao R, Cerutis D, Rojas P, Happe H, Murrin C, Pfeiffer R. Expression and regulation of brain metallothionein. Neurochem Int 27:1–22, 1995.
24. Maret W. Oxidative metal release from metallothionein via zinc-thiol/disulphide interchange. Proc Natl Acad Sci U S A 91:237–241, 1994.
25. Maret W. Metallothionein/disulphide interactions, oxidative stress, and the mobilization of cellular zinc. Neurochem Int 27:111–117, 1995.
26. Ebadi M, Hiramatsu M, Burke WJ, Folks DG, el-Sayed MA. Metallothionein isoforms provide neuroprotection against 6-hydroxy-dopamine-generated hydroxyl radicals and superoxide anions. Proc West Pharmacol Soc 41:155–158, 1998.
27. Ebadi M. Glutathione and metallothionein in neurodegeneration-neuroprotection of Parkinson's disease. Neuroendocrinol Lett 18: 111–122, 1998.
28. Sharma S, Ebadi M. An improved method for analyzing coenzyme Q homologues and multiple detection of rare biological samples. J Neurosci Methods 137:1–9, 2004.
29. Rojas P, Cerutis DR, Happe HK, Murrin JC, Hao R, Pfeiffer RF, Ebadi M. 6-Hydroxy-dopamine-mediated induction of rat brain MT-I mRNA. Neurotoxicology 17:323–334, 1996.
30. Rojas P, Hidalgo J, Ebadi M, Rios C. Changes of MT-I+II proteins in the brain after 1-methyl-4-phenylpyridinium administration in mice. Prog Neuropsychopharmacol Biol Psychiatry 24:143–154, 2001.
31. Rojas P, Rojas-Castaneda J, Vigueras, RM, Habeebu SS, Rojas C, Rios C, Ebadi M. MPTP decreases MT-I mRNA in mouse striatum. Neurochem Res 25:503–509, 2001.
32. Beckman JS, Koppenol WH. Nitric oxide, superoxide, and peroxynitrite: the good, the bad, and the ugly. Am J Physiol 271:C1424–C1437, 1996.
33. Brown RH. Amyotrophic lateral sclerosis. Recent insight from genetics and transgenic mice. Cell 80:687–692, 1995.
34. Beckman JS. Peroxynitrite verses hydroxyl radical: the role of nitric oxide in superoxide-dependent cerebral injury. Ann N Y Acad Sci 738: 69–75, 1994.
35. Radi R, Rodriguez M, Castro L, Telleri R. Inhibition of mitochondrial transport by peroxynitrite. Arch Biochem Biophys 308:89–95, 1994.
36. Sharma SK, Carlson E, Ebadi M. Neuroprotective actions of selegiline in inhibiting 1-methyl, 4-phenyl, pyridinium ion (MPP^+)-induced apoptosis in SK-N-SH neurons. J Neurocytology 32:329–343, 2003.
37. Ebadi M, Sharma S, Shavali S, El Refaey H. Neuroprotective actions of selegiline. J Neurosci Res 67:285–289, 2002.
38. Rohrer D, Nilaver G, Nipper V, Machida C. Genetically modified PC12 brain grafts: survivability and inducible nerve growth factor expression. Cell Transplant 5:57–68, 1996.
39. Lee HS, Park CW, Kim YS. MPP^+ increases the vulnerability to oxidative stress rather than directly mediating oxidative damage in human neuroblastoma cells. Exp Neurol 165:164–171, 2002.
40. Ebadi M, Leuschen MP, el Refaey H, Hamada FM, Rojas P. The antioxidant properties of zinc and metallothionein. Neurochem Int 29: 159–166, 1996.
41. Khatai L, Goessler W, Lorencova H, Zangger K. Modulation of nitric oxide mediated metal release from metallothionein by the redox state of glutathione in vitro. Eur J Biochem 271:2408–2416, 2004.